ChemComm

COMMUNICATION

View Article Online
View Journal | View Issue

Cite this: *Chem. Commun.*, 2014, **50**, 10244

Received 25th June 2014,
Accepted 16th July 2014

DOI: 10.1039/c4cc04835k

www.rsc.org/chemcomm

Formation of ultra-long nanoribbons by self-assembly of carbon dots and anionic oligomers for multi-colored fluorescence and electrical conduction†

Guiyang Zhang,‡[a] Manqing Yan,‡[a] Xiyao Teng,[a] Hong Bi,*[a] Yuyan Han,[b] Mingliang Tian[b] and Mingtai Wang*[c]

We report a facile and scalable synthesis of ultra-long (>100 μm) nanoribbons based on self-assembly of positively charged carbon dots (C-dots) and anionic oligomers of styrene and 4-styrenesulfonate (PS-PSS) in a mixture of ethanol and water (4/1, v/v). The obtained hybrid (PS-PSS)/C-dot nanoribbons show a multi-colored fluorescence and an electrical conductivity of 3.368 S m^{-1}.

Graphene nanoribbons (GNRs) are attracting more and more attention due to their appealing semiconducting properties, namely with a finite band gap in contrast to graphene which itself is a zero band gap semimetal.[1–6] Various 'top-down' routes offer limited control over edge structures and ribbon widths, which promotes an atomically precise 'bottom-up' chemical synthetic strategy based on cyclodehydrogenation of tailored polyphenylene precursors,[7–11] resulting in GNRs of broad absorption extended to the near-infrared region.[10,11] Nevertheless, the reported longest GNRs prepared by the bottom-up solution synthesis are only 200 nm in longitude,[11] and the rather high polydispersity of the polyphenylene precursors means that the resulting GNR products have a wide range of lengths.[12] Additionally, boron-doped GNRs prepared by a vacuum activation method are also 150–200 nm in length.[13] To date, there has been no report on the reliable fabrication of ultra-long (>1 μm) GNRs with a well-defined structure. Obviously, this task encounters some fundamental challenges in synthetic chemistry.

On the other hand, the assembly of quantum dots (QDs) in a geometrically well-defined fashion opens up opportunities to achieve one-dimensional (1D) architectures by using zero-dimensional (0D) nanodots as building blocks. Graphene quantum dots (GQDs), single or few-layer graphenes with a tiny size of only several nanometers, represent a new type of QDs.[14] Due to quantum confinement and edge effects, GQDs exhibit unique properties such as tunable fluorescence, high quantum yield (QY), and low cytotoxicity.[15,16] The hierarchically porous nanotube of graphene quantum dots (GQDs) has been prepared by electrophoresis deposition within a nanoporous anodic alumina template.[14] However, this template-based method is generally limited by a rather tedious post-synthesis process of removing the template with the risk of destroying the desired structure. In contrast, the wet chemical methods based on self-assembly can offer simple, economical and scalable routes to such 1D nanosystems.[17] For example, a successful self-assembly of *o*-phenylenediamine (oPD) oligomers into 1D structures from a $AgNO_3$-oPD aqueous solution was a cooperative result of π–π interaction and electrostatic repulsion.[18] Moreover, by combining organic and inorganic nanodots in a controlled manner, the complexity and functionality can be considerably enhanced. New properties and hierarchical architectures of 1D nanomaterials, which do not exist in any building block, can be attained through the interfacial interaction among the organic and/or inorganic phases in a 1D hybrid.[19] Recently, a single inorganic–organic hybrid nanowire was found with ambipolar photoresponse,[20a] and luminescent 3D microstructures were formed by carbon quantum dots (C-dots)–polypeptide hybrids and their self-assemblies.[20b]

Here we demonstrate a facile and scalable synthesis of ultra-long (>100 μm) nanoribbons with a multi-colored fluorescence and a high electrical conductivity based on self-assembly of positively charged C-dots and anionic oligomers of styrene (St) and 4-styrenesulfonic acid sodium salt (NaSS) in a mixture of ethanol and water (4/1, v/v), so the obtained nanoribbons are

[a] *College of Chemistry and Chemical Engineering, Anhui University, Hefei, 230601, China. E-mail: bihong@ahu.edu.cn*
[b] *High Magnetic Field Laboratory, Chinese Academy of Sciences, Hefei 230031, China*
[c] *Institute of Plasma Physics, Chinese Academy of Sciences, Hefei 230031, China. E-mail: mtwang@ipp.ac.cn*

† Electronic supplementary information (ESI) available: AFM and TEM images of the C-dots, experimental details of preparation and characterization of C-dots and (PS-PSS)/C-dot nanoribbons, supplemental TEM and fluorescence microscopy images of the (PS-PSS)/C-dot nanoribbons, ^{1}H NMR spectrum of the (PS-PSS)/C-dot nanoribbons, MALDI-TOF mass spectrum of the remanent of the (PS-PSS)/C-dot nanoribbons after being dissolved in H_2O, GPC traces of the (PS-PSS)/C-dot nanoribbons and PS-PSS microspheres, the micrographs of an individual nanoribbon between two electrodes and in an OFET device, and SEM and TEM images of the Ag-(PS-PSS)/C-dot nanoribbons. See DOI: 10.1039/c4cc04835k

‡ These authors contributed equally to this work.

denoted as (PS-PSS)/C-dots. Although each nanoribbon is an inorganic–organic 1D hybrid, it has a very ordered and morphologically-defined structure that was supported by infrared, Raman, MALDI-TOF mass spectroscopy, ultraviolet-visible (UV-vis) absorption and nuclear magnetic resonance (NMR) spectroscopies.

The C-dots of *ca.* 2 nm in size as shown in Fig. S1 in ESI† were prepared by pyrolysis of konjac flour (KF) as previously reported in our lab,[21] and the as-prepared C-dots possessed a positive Zeta potential of *ca.* +3.8 mV (see Experimental details, ESI†). The preparation of the (PS-PSS)/C-dot nanoribbons included modified precipitation copolymerization of NaSS and St by adding C-dots into the system after the polymerization proceeded for a few minutes, which is similar to generating the Au–PS hybrid particles reported by Ohnuma *et al.* in 2009.[22] It includes two stages as illustrated in Fig. 1. First, NaSS and excessive potassium persulphate (KPS) were dissolved in a mixture of ethanol and water (4/1, v/v) under stirring and then the mixture was heated to 70 °C. Very shortly, St was added into the mixture to produce PS-PSS oligomers under KPS initiation at 70 °C for 2 minutes. Second, a small amount (7.26 wt%) of C-dots in ethanol was added dropwise into the mixture to induce the self-assembly and formation of (PS-PSS)/C-dot nanoribbons, which was the white precipitate collected from the reactant system (see Experimental details, ESI†). As a control, only PS-PSS microspheres were obtained when the C-dots were not added into the reaction system (Fig. S2, ESI†).

Transmission electron microscopy (TEM) (Fig. 2A) and scanning electron microscopy (SEM) (Fig. 2B) images show that the obtained nanoribbons have a width of 1–2 μm and an ultra-long length of tens to hundreds of micrometers. The atomic force microscopy (AFM) image (Fig. S3c and d, ESI†) reveals that the surface of nanoribbons is convex with a thickness of *ca.* 80–120 nm. It should be noted that the nanoribbons have not been stained with any heavy metals when preparing the specimen for TEM observations, but the high-energy electron beam of 200 kV from the electron microscope will destroy the microstructures of the nanoribbons in a very short time (see Fig. S4, ESI†), so the TEM pictures should be taken very quickly. The high-resolution TEM (HRTEM) image in Fig. 2C shows that there are many bright areas with prominent zigzag patterns on a single nanoribbon, where the selected area electron diffraction (SAED) pattern indicates its single crystallinity with a lattice distance

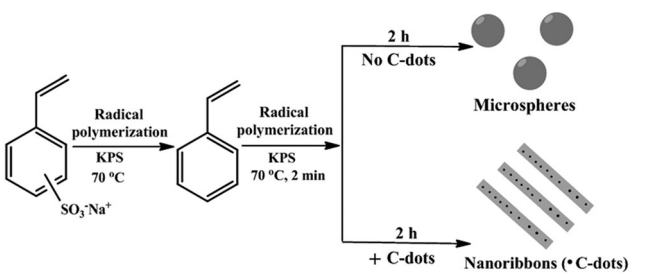

Fig. 1 Schematic preparation procedures of (PS-PSS)/C-dot nanoribbons and PS-PSS microspheres, respectively.

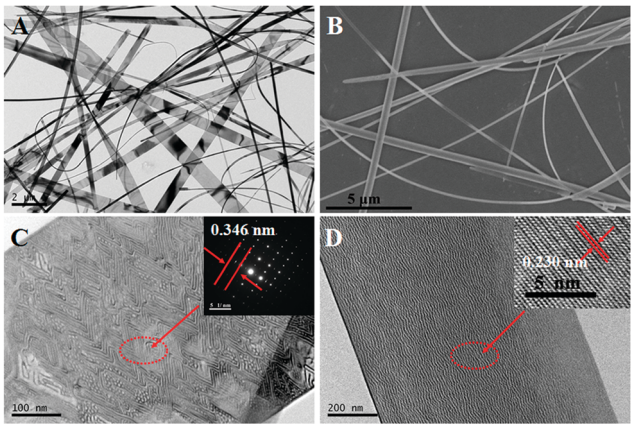

Fig. 2 (A) TEM and (B) SEM images of (PS-PSS)/C-dot nanoribbons. (C) HRTEM image of a single nanoribbon, the inset shows the SAED pattern. (D) HRTEM image of another single nanoribbon, the inset shows the corresponding lattice fringes of the area within the dotted circle.

of 0.346 nm, in accordance with the inter-layer distance of graphite. In addition, Fig. 2D shows another HRTEM image of one more nanoribbon exhibiting clear lattice fringes with a regular spacing of 0.230 nm (inset to Fig. 2D), which is in agreement with an (1120) in-plane lattice spacing of C-dots of 0.213 nm (Fig. S1c, ESI†) or 0.217 nm as previously reported.[21] This result indicates the presence of C-dots in the nanoribbons, and the zigzag pattern is a typical feature of oriented superstructures of assembled C-dots and oligomers (see also Fig. S3b, ESI†), which reveals that the nanoribbon is internally heterogeneous owing to inorganic–organic hybrids.[23]

Furthermore, the chemical components of the nanoribbons were characterized by employing FT-IR, Raman, ^{1}H NMR and MALDI-TOF mass spectroscopy. Fig. 3A shows FT-IR spectra of

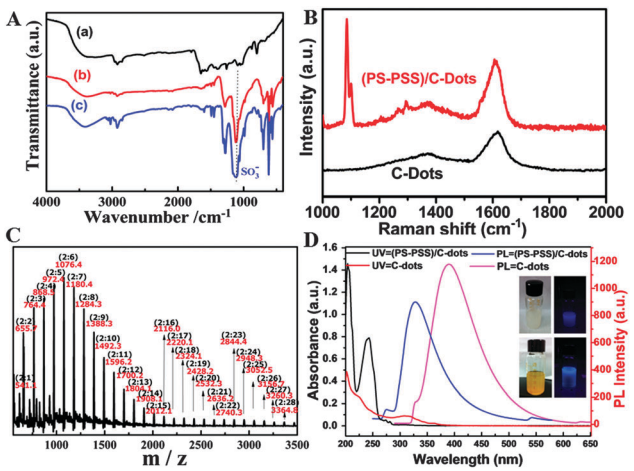

Fig. 3 (A) FT-IR spectra of (a) C-dots, (b) PS-PSS microspheres and (c) (PS-PSS)/C-dot nanoribbons. (B) Raman spectra of (PS-PSS)/C-dot nanoribbons and C-dots (λ_{ex} = 325 nm). (C) MALDI-TOF mass spectrum (negative mode) of the (PS-PSS)/C-dot nanoribbons. (D) UV-Vis absorption and photoluminescence spectra of the (PS-PSS)/C-dot nanoribbons and the C-dots, the inset shows the blue fluorescence of (PS-PSS)/C-dot nanoribbons (up) and C-dots (down) in ethanol under UV light (λ_{ex} = 365 nm).

C-dots, PS-PSS microspheres and the as-prepared nanoribbons. Although the FT-IR spectrum of C-dots is essentially featureless, FT-IR spectra of both PS-PSS microspheres and the nanoribbons are quite similar and informative, particularly exhibiting a strong $-SO_3^-$ absorption feature at 1081 cm^{-1}, which confirms the presence of the PSS segment in the nanoribbon. Meanwhile four characteristic peaks at 699, 757, 1453 and 1493 cm^{-1} assigned to unsubstituted phenyl rings indicate the co-existence of the PS segment in the nanoribbon.[24] The Raman spectrum of the nanoribbons (Fig. 3B) shows a prominent peak at 1084 cm^{-1} of PS,[25] and the typical D (at 1376 cm^{-1}) and G (at 1608 cm^{-1}) bands of graphitic materials.[26] It is well-known that the intensity ratio of the D and G bands (I_D/I_G) is a measurement of the extent of the disorder, and the ratio of sp^3/sp^2 carbon atoms.[26,27] The I_D/I_G value of our nanoribbons is 0.50, which is obviously smaller than that in the original C-dots (0.77). The main reason is that after the self-assembly of PS-PSS and the C-dots, the introduction of a large amount of sp^2 carbon atoms in benzene groups of PS and PSS will increase the content of sp^2 carbon atoms in the ribbons, thus reducing the ratio of sp^3/sp^2 carbon atoms and consequently decreasing I_D/I_G. Moreover, the nanoribbons were found to be soluble in organic solvents such as $CHCl_3$ and THF, and then C-dots would be released from the nanoribbons. As shown in Fig. S5, ESI,† an entire nanoribbon exhibits bright blue, green, and red fluorescence under a fluorescent microscope, however, many fluorescent aggregated dots will be seen when the nanoribbons dissolved in THF. This result demonstrates that the C-dots locate along a whole nanoribbon acting as important building blocks. Fig. S6 (ESI†) shows the ^1H NMR spectrum of the supernatant after the nanoribbons dissolved in D-substituted chloroform ($CDCl_3$), confirming three features of PS at (a) δ = 6.0–7.25, (b) δ = 1.42, and (c) δ = 1.80 ppm. Moreover, a little white flocculent precipitate will still be seen when the nanoribbons are dissolved in H_2O, confirming the presence of the hydrophobic PS segment in the nanoribbons. Fortunately, the nanoribbons cannot be dissolved in ethanol, and they have a good dispersion in ethanol which can be stable at room temperature even after a few days (Fig. S7, ESI†). Therefore, both suspensions of nanoribbons and the original C-dots in ethanol show blue fluorescence under UV light (λ_{ex} = 365 nm, inset to Fig. 3D). The UV-Vis spectrum of the nanoribbons in ethanol possesses a distinct strong absorption of the PSS segment at 250 nm.[28,29] More interestingly, the fluorescence emission spectrum of the suspended nanoribbons blue shifts obviously compared to that of the primary C-dots (Fig. 3D), this up-conversion PL phenomenon probably resulted from the interaction between PS-PSS oligomers and C-dots, since the up-conversion PL feature was also found in surface passivated C-dots attributed to the multiphoton active process.[30]

The aforementioned results indicate that the nanoribbons are composed of C-dots and PS-PSS oligomers. Furthermore, molecular weights and polydispersity of the oligomers have been determined by gel permeation chromatography (GPC) using THF as a mobile phase (Fig. S8, ESI†). However, for these low-molecular-weight samples GPC is not a very precise method to determine the molecular weight.[18] Thus, the more accurate molecular weights of the oligomers can be obtained by the MALDI-TOF mass spectroscopy technique. The negative-mode MALDI-TOF spectrum of (PS-PSS)/C-dot nanoribbons (Fig. 3C) gives a similar molecular weight distribution (M_n = 1408.69 Da, M_w = 1693.32 Da, PDI = 1.20) to the GPC traces in Fig. S8 (ESI†). The interval between two neighboring peaks is 104, equal to the molecular weight of St.[31a,b] The observed mass of the peaks, for example, the major peak at 1076.4 Da in Fig. 3C, corresponds to those PS-PSS oligomer chains with 6 St repeating units and 2 NaSS units plus one end group (–OH) and Na^+ from the cationizing agent NaTFA (see Experimental details, ESI†), thus those oligomer chains symbolized as 2 : 6. In addition, Fig. S9 (ESI†) shows the MALDI-TOF mass spectrum of the remanent of the (PS-PSS)/C-dot nanoribbons after being dissolved in H_2O, which confirms that the remanent is mainly hydrophobic PS-PSS with longer PS segments and thus has higher molecular weights since the PS-PSS oligomers with shorter PS segments are soluble in water. Furthermore, the Zeta potential of the nanoribbons in the mixture of ethanol and water (4/1, v/v) was measured to be about −18.2 mV, which demonstrates the polyelectrolyte character of the PS-PSS nanoribbons.

We have found that C-dots play an important role in formation of the nanoribbons. In fact, each component is indispensable in the present case since no nanoribbons can be obtained if the reaction feed lacks any of the three reagents of St, NaSS and C-dots. We further found that the thickness of nanoribbons would increase upon prolonging the self-assembly time to 3 h, together with the change in the nanoribbon morphology (Fig. S10a, ESI†). When the self-assembly time increased to 4 h, the nanoribbons became poorly crystallized with many stacking faults due to the layer-by-layer self-assembly (Fig. S10b, ESI†). Therefore, it is proposed that the architecture of the nanoribbon is built on C-dots and PS-PSS oligomer blocks, which combine into a repeating unit and then each unit self-assembled into an ordered 1D nanostructure based on an electrostatic interaction between a positively charged C-dot and the negatively charged PS-PSS oligomer, and the C-dots stack along the length direction with intermediate polymer layers, as illustrated in Fig. S11 (ESI†).

The fluorescence microscopy images shown in Fig. 4 indicate that the nanoribbons have a multi-color fluorescent property. Selecting Rhodamine 6G as a standard, the calculated QYs of the C-dots and the nanoribbons in ethanol according to photoluminescence (PL) spectra in Fig. 3D were 18% and 17%,

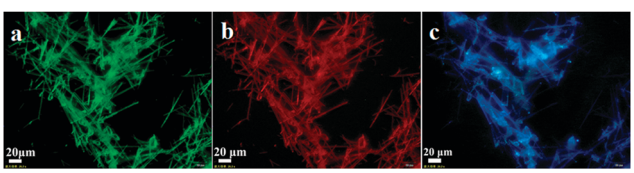

Fig. 4 Fluorescence microscopy images of the (PS-PSS)/C-dot nanoribbons in (a) the green channel (ex. 405 nm and em. 480–520 nm), (b) the red channel (ex. 534 nm, em. 580–620 nm) and (c) the blue channel (ex. 385 nm, em. 470 nm), respectively.

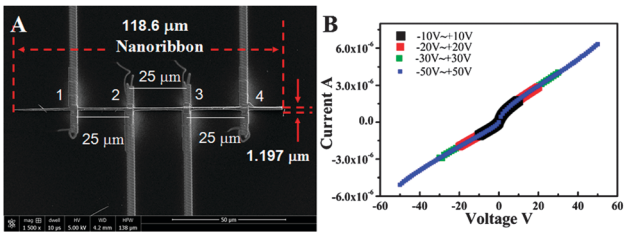

Fig. 5 (A) The micrograph of a single (PS-PSS)/C-dot nanoribbon bridging two 25 μm-spaced Pt electrodes. (B) *I–V* characteristics of the (PS-PSS)/C-dot nanoribbons by measuring variations in four different voltage ranges.

respectively (the procedures for measuring the QYs are provided in Experimental details, ESI†). The strong PL intensity as well as an up-conversion property (as shown in Fig. 3D) of the nanoribbons make them promising for the application in optical devices and sensors.

The electrical characteristic of the (PS-PSS)/C-dot nanoribbons was obtained with a table-top cryogenic probe station (Lake Shore, Model TTPX) using a Keithley 2400 sourcemeter under vacuum conditions. As shown in Fig. 5A, a randomly selected nanoribbon was carefully pressed onto two 25 μm-spaced Pt electrodes in an OFET device (Fig. S12, ESI†), where a small beam current of 2.3 nA was applied under 30 kV acceleration voltage in order to avoid the milling of the nanoribbon. The conductivity obtained from the quasi-linear range from −40 V to −20 V in the *I–V* curves (shown in Fig. 5B) was estimated on the basis of the known nanoribbon dimensions (Fig. S12, ESI†) to be 3.368 S m^{-1}, which is 3 orders of magnitude more compared to the conductivity of graphene quantum dots in air.[32] The conductivity of the (PS-PSS)/C-dot nanoribbons is in accordance with that in poly(3,4-ethylenedioxythiophene) (PEDOT):PSS, which is the most widely applied transparent organic semiconductor in organic electronics and conductivity typically <10 S cm^{-1} is used.[33]

In summary, ultralong (PS-PSS)/C-dot nanoribbons were prepared by self-assembly of C-dots and PS-PSS oligomers on the basis of electrostatic interactions. The obtained nanoribbons exhibit not only a multi-colored fluorescence but also an electrical conductivity of 3.368 S m^{-1}. The strong PL intensity and suitable conductivity make the (PS-PSS)/C-dot nanoribbons more advantageous and promising to be applied in organic light emitting diode pixels and millimeter-sized lab scale photovoltaic cells. Moreover, the obtained nanoribbons can be used as feasible templates to prepare other multifunctional 1D nanostructures such as Ag-(PS-PSS)/C-dot nanobelts (see Fig. S13, ESI†).

This work was financed by the 211 Project of Anhui University, the National Natural Science Foundations of China (Grant No. 51272002), the Anhui Provincial Natural Science Foundation (1208085ME87), and the Technology Foundation for Selected Overseas Chinese Scholar, the Ministry of Personnel of China (No. [2013]-385). All co-authors thank the Key Laboratory of Environment-Friendly Polymer Materials of Anhui Province.

Notes and references

1 Y.-W. Son, M. L. Cohen and S. G. Louie, *Nature*, 2006, **444**, 347.
2 M. Y. Han, B. Özyilmaz, Y. Zhang and P. Kim, *Phys. Rev. Lett.*, 2007, **98**, 206805.
3 X. Li, X. Wang, L. Zhang, S. Lee and H. Dai, *Science*, 2008, **319**, 1229.
4 (*a*) D. V. Kosynkin, A. L. Higginbotham, A. Sinitskii, J. R. Lomeda, A. Dimiev, B. K. Price and J. M. Tour, *Nature*, 2009, **458**, 872; (*b*) L. Jiao, L. Zhang, X. Wang, G. Diankov and H. Dai, *Nature*, 2009, **458**, 877.
5 A. H. C. Neto, F. Guinea, N. M. R. Peres, K. S. Novoselov and A. K. Geim, *Rev. Mod. Phys.*, 2009, **81**, 109.
6 (*a*) X. Jia, M. Hofmann, V. Meunier, B. G. Sumpter, J. Campos-Delgado, J. M. Romo-Herrera, H. Son, Y.-P. Hsieh, A. Reina, J. Kong, M. Terrones and M. S. Dresselhaus, *Science*, 2009, **323**, 1701; (*b*) K. A. Ritter and J. W. Lyding, *Nat. Mater.*, 2009, **8**, 235.
7 X. Yang, X. Dou, A. Rouhanipour, L. Zhi, H. J. Räder and K. Müllen, *J. Am. Chem. Soc.*, 2008, **130**, 4216.
8 J. Cai, P. Ruffieux, R. Jaafar, M. Bieri, T. Braun, S. Blankenburg, M. Muoth, A. P. Seitsonen, M. Saleh, X. Feng, K. Müllen and R. Fasel, *Nature*, 2010, **466**, 470.
9 L. Dössel, L. Gherghel, X. Feng and K. Müllen, *Angew. Chem., Int. Ed.*, 2011, **50**, 2540.
10 M. G. Schwab, A. Narita, Y. Hernandez, T. Balandina, K. S. Mali, S. De Feyter, X. Feng and K. Müllen, *J. Am. Chem. Soc.*, 2012, **134**, 18169.
11 A. Narita, X. Feng, Y. Hernandez, S. A. Jensen, M. Bonn, H. Yang, I. A. Verzhbitskiy, C. Casiraghi, M. R. Hansen, A. H. R. Koch, G. Fytas, O. Ivasenko, B. Li, K. S. Mali, T. Balandina, S. Mahesh, S. De Feyter and K. Müllen, *Nat. Chem.*, 2014, **6**, 126.
12 C. Scott Hartley, *Nat. Chem.*, 2014, **6**, 91.
13 M. Xing, W. Fang, X. Yang, B. Tian and J. Zhang, *Chem. Commun.*, 2014, **50**, 6637.
14 H. Cheng, Y. Zhao, Y. Fan, X. Xie, L. Qu and G. Shi, *ACS Nano*, 2012, **6**, 2237.
15 Y. Sun, S. Wang, C. Li, P. Luo, L. Tao, Y. Wei and G. Shi, *Phys. Chem. Chem. Phys.*, 2013, **15**, 9907.
16 L. Li, G. Wu, G. Yang, J. Peng, J. Zhao and J.-J. Zhu, *Nanoscale*, 2013, **5**, 4015.
17 S. M. Watson, M. A. Galindo, B. R. Horrocks and A. Houlton, *J. Am. Chem. Soc.*, 2014, **136**, 6649.
18 X. Sun, S. Dong and E. Wang, *Macromol. Rapid Commun.*, 2005, **26**, 1504.
19 J. Yuan, Y. Xu and A. H. E. Müller, *Chem. Soc. Rev.*, 2011, **40**, 640.
20 (*a*) J. Yoo, J. Pyo and J.-H. Je, *Nanoscale*, 2014, **6**, 3557; (*b*) D. Mazzier, M. Favaro, S. Agnoli, S. Silvestrini, G. Granozzi, M. Maggini and A. Moretto, *Chem. Commun.*, 2014, **50**, 6592.
21 X. Teng, C. Ma, C. Ge, M. Yan, J. Yang, Y. Zhang, P. C. Morais and H. Bi, *J. Mater. Chem. B*, 2014, **2**, 4631.
22 A. Ohnuma, E. C. Cho, P. H. C. Camargo, L. Au, B. Ohtani and Y. Xia, *J. Am. Chem. Soc.*, 2009, **131**, 1352.
23 M. Huang, U. Schilde, M. Kumke, M. Antonietti and H. Cölfen, *J. Am. Chem. Soc.*, 2010, **132**, 3700.
24 Z. Shi and S. Holdcroft, *Macromolecules*, 2005, **38**, 4193.
25 K. J. McKee, M. W. Meyer and E. A. Smith, *Anal. Chem.*, 2012, **84**, 9049.
26 H. Li, Z. Kang, Y. Liu and S.-T. Lee, *J. Mater. Chem.*, 2012, **22**, 24230.
27 P. Luo, Z. Ji, C. Li and G. Shi, *Nanoscale*, 2013, **5**, 7361.
28 S. Stankovich, R. D. Piner, X. Chen, N. Wu, S. T. Nguyen and R. S. Ruoff, *J. Mater. Chem.*, 2006, **16**, 155.
29 C. S. Lao, M.-C. Park, Q. Kuang, Y. Deng, A. K. Sood, D. L. Polla and Z. L. Wang, *J. Am. Chem. Soc.*, 2007, **129**, 12096.
30 S. Zhu, J. Zhang, S. Tang, C. Qiao, L. Wang, H. Wang, X. Liu, B. Li, Y. Li, W. Yu, X. Wang, H. Sun and B. Yang, *Adv. Funct. Mater.*, 2012, **22**, 4732.
31 (*a*) X. Wang, J. Xia, J. He, F. Yu, A. Li, J. Xu, H. Lu and Y. Yang, *Macromolecules*, 2006, **39**, 6898; (*b*) L.-W. Zhu, Y. Ou, L.-S. Wan and Z.-K. Xu, *J. Phys. Chem. B*, 2014, **118**, 845.
32 P. Gao, K. Ding, Y. Wang, K. Ruan, S. Diao, Q. Zhang, B. Sun and J. Jie, *J. Phys. Chem. C*, 2014, **118**, 5164.
33 A. J. Oostra, K. H. W. van den Bos, P. W. M. Blom and J. J. Michels, *J. Phys. Chem. B*, 2013, **117**, 10929.